Dynamic prediction of optical and chromatic performances for a light-emitting diode array based on a thermal-electrical-spectral model

Fan, Jiajie; Chen, Wei; Yuan, Weiyi; Fan, Xuejun; Zhang, Guoqi

DOI
10.1364/OE.387660

Publication date
2020

Document Version
Final published version

Published in
Optics Express

Citation (APA)
Fan, J., Chen, W., Yuan, W., Fan, X., & Zhang, G. (2020). Dynamic prediction of optical and chromatic performances for a light-emitting diode array based on a thermal-electrical-spectral model. *Optics Express*, *28*(9), 13921-13937. https://doi.org/10.1364/OE.387660

Research Article | Vol. 28, No. 9 / 27 April 2020 / Optics Express 13921
Optics EXPRESS

Dynamic prediction of optical and chromatic performances for a light-emitting diode array based on a thermal-electrical-spectral model

JIAJIE FAN,[1,2,3,4,*] WEI CHEN,[2,3] WEIYI YUAN,[2] XUEJUN FAN,[5] AND GUOQI ZHANG[4]

[1]Academy for Engineering and Technology, Fudan University, Shanghai 200433, China
[2]College of Mechanical and Electrical Engineering, Hohai University, Changzhou 213022, China
[3]Changzhou Institute of Technology Research for Solid State Lighting, Changzhou 213164, China
[4]EEMCS Faculty, Delft University of Technology, 2628 Delft, The Netherlands
[5]Department of Mechanical Engineering, Lamar University, Beaumont, TX 77710, USA
*jay.fan@connect.polyu.hk

Abstract: Light-emitting diode (LED) arrays have attracted increased attention in the area of high power intelligent automotive headlamps because of their superiority in disposing of the power limit of an individual LED package and controllably luminous intensity and illumination pattern. The optical and chromatic performances of an LED array do not equal to the sum of individual LED packages' performances, as the thermal interactions between individual LED packages can't be ignored in the actual application. This paper presents a thermal-electrical-spectral (TES) model to dynamically predict the optical and chromatic performances of the LED array. The thermal-electrical (TE) model considering the thermal coupling effect in the LED array is firstly proposed to predict the case temperature of each individual LED package, and the Spectral power distributions (SPDs) of individual LED package is then decomposed by the extended Asym2sig model to extract the spectral characteristic parameters. Finally, the experimental measurements of the designed LED arrays operated under usage conditions are used to verify the TES model. Some validation case studies show that the prediction accuracy of the proposed TES model, which is expressed as a quadratic polynomial function of current and case temperature, can be achieved higher than 95%. Therefore, it can be concluded that this TES model offers a convenient method with high accuracy to dynamically predict the optical and chromatic performances of LED arrays at real usages.

1. Introduction

In recent decades, light-emitting diode (LED), as one of new generation solid-state lighting (SSL) light sources, draws worldwide attention in lighting and beyond-lighting industry, as it benefits in small volume, low power consumption and environmental friendship [1]. With the advantages over other conventional light sources such as incandescent bulbs, halogen lamps, xenon HID lamps, LED has progressed rapidly to be applied in general lighting [2] and many special fields such as plant lighting [3], automotive lighting [4], healthcare lighting [5] and visible light communication (VLC) [6]. However, the luminous intensity of a single LED package can't satisfy the high power and high illumination application because of the power limit of an individual LED package and its efficiency droop effect [7–9]. So, the LED array prepared by several arranged LED individuals [10–12] is emerged in high power applications, such as street lighting, automotive lighting, detector lighting, etc. Moreover, it also can achieve adjusting of the illumination pattern and luminous intensity by controlling each LED individuals independently [13].

#387660 https://doi.org/10.1364/OE.387660
Journal © 2020 Received 10 Jan 2020; revised 22 Feb 2020; accepted 2 Apr 2020; published 23 Apr 2020

Optics EXPRESS

Normally, LED converts a part of electric energy to light, meanwhile, most of electric energy is converted to heat leading to high junction temperature. The luminous efficacy of LED is always deteriorated when it operates under high temperature and high current condition [14]. With increase the current of LED, more electric energy is consumed as its efficiency droop effect. Besides, high junction temperature also accelerates the lumen degradation. Thus, thermal management becomes one of critical research focuses for LEDs from chip to systems [1,4,15–18]. The optical and chromatic performances of an individual LED package is directly influenced by its driven current and surrounding temperature. The temperature distribution of a LED array will be affected more from the thermal coupling effect deriving from the adjacent LED individuals. Therefore, the prediction of temperature, optical and chromatic performances for a LED array encounters challenges from the complex impact factors, such as driven current, application temperature, electrical-thermal coupling of a single LED and thermal coupling between LED neighborhoods [19]. There have been some researches on thermal coupling effect by using the thermal resistance matrix method, that provides a theoretical guidance on the thermal management of LED array [20–22]. Lu et al. [19] proposed a new and effective method to estimate the thermal resistance matrix of a LED array. However, they only used the thermal resistance matrix to predict the temperature rise of the LED array, and an extra sensor was needed to measure the temperature of reference position.

In the prediction of optical performances for white LED (WLED), Hui et al. [23] proposed a general photo-electro-thermal (PET) theory for WLED which can relate the luminous flux with input power and thermal resistance. In this proposed PET model, the suitable input power could be selected for WLED under the certain thermal design. After that, they updated this general PET theory with the new coefficients k_e and k_h [24]. Moreover, Chen et al. [25] used the PET theory to estimate the optical power, wall-plug efficiency and the coefficient of heat-dissipation for WLEDs and they also combined the PET theory to a photo-detector system to estimate the dynamic/transient optical power and junction temperature for WLEDs [26]. Currently, they also improved the full PET theory to predict the fall and rise time of luminous flux for WLEDs by adding the photodiode as the measurement component [27]. Combining the electrical-thermal model, electrical-luminous model and thermal-luminous model together, the thermal–electrical–luminous model derived from the automatic control theory was proposed by Huang et al. to study the dynamic performances of RGB LED [28]. Lin et al. [29] proposed a novel method based down-conversion luminescence efficiency (DCLE) concept, connecting the total absorption ratio of phosphor, to estimate the conversion efficiency of phosphor accurately of phosphor converted WLED. In addition, some researchers [30–33] built the equivalent circuit to simulate the photo-electro-thermal coupling effect for WLEDs, and they used the Simulation Program with Integrated Circuit Emphasis (SPICE) to simulate the junction temperature, luminous flux or power density of WLEDs. Besides optical performances, the chromatic performances, such as correlated color temperature (CCT), chromaticity coordinate and color rendering index (CRI), are also essential metrics for characterizing the WLEDs. In the recent years, some researchers realized that color shift became another critical failure mode impacting the service life of the WLEDs applied in high color rending area [34,35]. And there have been some models proposed aiming to predict the chromatic performance of WLEDs. For instance, Chen et al. [36] linked the CCT to luminous flux for a WLED array with two types of WLEDs based on the PET theory. The PET theory was combined with spectral power distribution (SPD) by them to predict the CCT and CRI [37]. Ye et al. [38] proposed an electrical–thermal–luminous–chromatic model, combining the electrical-thermal model and the thermal-luminous-chromatic model, to predict the chromatic performance of WLED under certain operation temperatures. Fu et al. [39] provided an empirical model based on the band gap transition scheme described by the Gaussian functions and experimentally verified the accuracy in prediction of chromatic characteristics for WLED. However, most of current researches develop models for the individual WLED packages,

Optics EXPRESS

few of them consider the thermal coupling effect in predicting of the optical and chromatic performances for LED array.

To achieve dynamic prediction of the optical and chromatic performances for LED array under different operation conditions, the thermal-electrical-spectral (TES) model that combines the Thermal-Electrical (TE) model with the SPD model is proposed. The TE model considers the thermal coupling effect with the purpose to predict the temperature distribution of LED array. The SPD model is developed to disassemble, reconstruct and superimpose the SPDs aiming to achieve the dynamic prediction of optical and chromatic performances for LED array. Lastly, the prediction accuracy of proposed TES model under different operation conditions will be validated. The remainder of the paper is organized as follows: Section 2 introduces the test samples and experiments designed in this paper. Section 3 proposes and implements the TE model and TES model. Section 4 discusses the prediction accuracy. Finally, section 5 proposes the concluding remarks.

2. Test samples and experiments

In this section, the designs of test sample and experiments used in this paper are introduced.

2.1. Test samples

As shown in Fig. 1(a), the phosphor converted white LED (pc-WLED) chip scale package (CSP) used in this study is composed of an InGaN LED chip (SIRIUS-KIK3014) with the size of 0.78*0.38*0.14mm as the light emitter and the phosphor/silicone composite with the size of 1.2*1.0*0.5mm as the light and color converter. The phosphor/silicone composite is a mixture of silicone, yellow phosphor: YAG: Ce^{3+} (Intematix YAG-04) and red phosphor: $CaAlSiN_3:Eu^{2+}$ (Intematix R6535). The rated current and voltage of test sample are 120mA and 3.0V, respectively. The LEDs are soldered on an aluminum printed circuit board (PCB) with the size of 60*60*1.6mm, named Sample LED1, Sample LED4, Sample LED6, Sample LED9, as shown in Fig. 1(b). The distance of two adjacent LEDs is 5mm at both rows and columns.

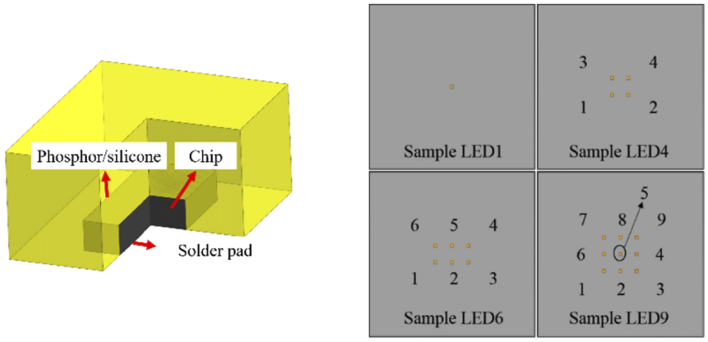

Fig. 1. Schematic diagram of (a) pc-WLED CSP and (b) LED array test samples used in this study.

2.2. Experimental and simulation setups

As shown in Fig. 2, the temperature distributions of test samples were collected by a thermal measurement setup, which contains an infrared camera (Model: Fluke Ti55FT with the accuracy of ± 2°C) and a thermal control platform to control the PCB temperature (Model: Everfine LED-220T). The integrating sphere test system with thermal control platform (Model: Everfine

Optics EXPRESS

HASS2000) was used to acquire photoelectric and chromatic parameters and SPD of test samples. The ambient temperature of all experiments and stimulations are set as 22 °C.

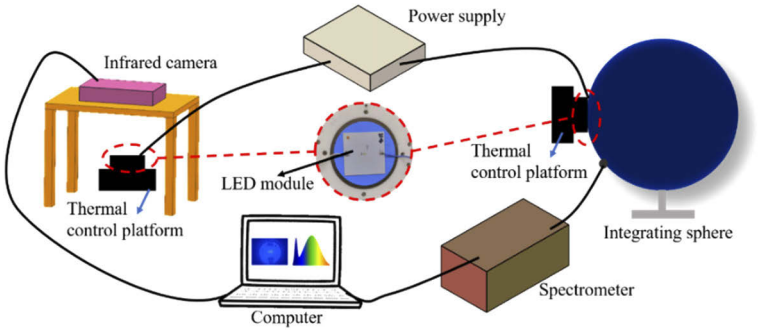

Fig. 2. Illustration the experimental setups for photoelectric parameters, SPD, and temperature measurements.

The thermal simulation based on the Fine Element Analysis (FEA) used in this study was conducted in Autodesk CFD 2018 to estimate the case temperatures of test samples. The key material parameters are listed in Table 1 and Table 2. The density of air flow changes with the environment controlled by the equation of state.

Table 1. The assumed Thermal Resistance Used in The FEA Simulation

Items	Descriptions
Thermal resistance of LED	From the junction to the PCB including the solder layer: 16 K/W
Thermal contact resistance	Between the underside of the LED and upside of PCB: 0.5 cm^2·K/W

Table 2. The Key Material Parameters Used in The FEA Simulation

Materials	Density (g/cm^3)	Thermal conductivity (W/cm·K)	Specific heat (J/g·K)
Air flow	/	2.563×10^{-4}	1.004
PCB	3.89	1.109	0.454

3. Modeling and implement

In this section, the Thermal-Electrical model and Thermal-Electrical-Spectral model are proposed and implemented.

3.1. Thermal-electrical modeling

For the encapsulating material with low thermal conductivity ~ 1×10^{-4} W/cm·K, it is assumed that all the heat is transferred to the heatsink through heat conduction, then the heat is dissipated to the ambient through heat convection on the surface of heatsink. The heat transfer path of an individual LED is showed in Fig. 3(a), and its equivalent thermal resistance network can be modeled as indicated in Fig. 4(a). According to the thermal resistance theory, the case temperature can be calculate using Eq. (1).

$$T_c = T_a + P_{th}(R_a + R_b) \tag{1}$$

where T_a is ambient temperature (22°C), R_a is the thermal-conduction resistance between the LED and PCB, R_b is the thermal-convection resistance between the heatsink and ambient. Because

Optics EXPRESS

the thermal power P_{th} includes two parts: (1) the heat energy generated from the blue chip and (2) the energy generated from self-heating of phosphor, the maximum temperature at surface of LED is assumed as the case temperature used in this paper.

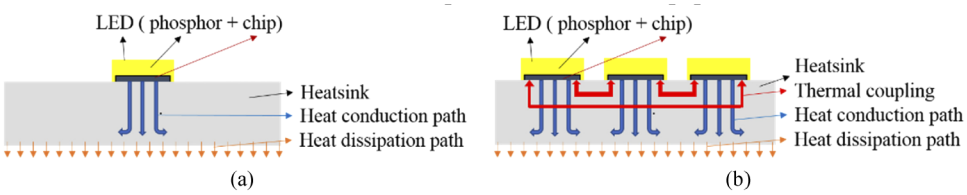

Fig. 3. Schematic diagram of (a) pc-WLED CSP and (b) LED array test samples used in this study.

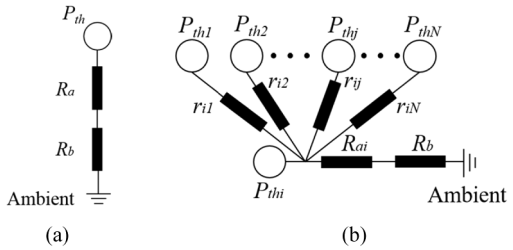

Fig. 4. Equivalent thermal resistance network in (a) an individual LED and (b) a LED array

In a LED array, as shown in Fig. 3(b), all LEDs transfer the heat to the heatsink, then all heat from the heatsink is dissipated to the ambient. Meanwhile, each LED is thermally influenced by the neighborhoods, resulting the rise of its case temperature, which is called the thermal couple effect. Thermal resistance network of a LED array is illustrated in Fig. 4(b) and its case temperature can be calculated by using Eq. (2).

$$T_{ci} = T_a + P_{thi}(R_{ai} + R_b) + \Delta T_{ci} \tag{2}$$

where T_i, P_{thi}, ΔT_{ci} are the case temperature of i^{th} LED, the thermal power of i^{th} LED and the case temperature rise caused by thermal coupling effect of other LEDs respectively. The ΔT_c can be calculated using Eq. (3).

$$\Delta T_c = \begin{pmatrix} \Delta T_{c1} \\ \Delta T_{c2} \\ \cdots \\ \Delta T_{cN} \end{pmatrix} = \begin{pmatrix} 0 & r_{12} & \cdots & r_{1N} \\ r_{21} & 0 & \cdots & r_{2N} \\ \vdots & \vdots & \ddots & \vdots \\ r_{N1} & r_{N2} & \cdots & 0 \end{pmatrix} \begin{pmatrix} P_{th1} \\ P_{th2} \\ \cdots \\ P_{thN} \end{pmatrix} \tag{3}$$

where the r is the thermal coupling constant which represents the degree of thermal couple effect. Combining Eq. (2) and Eq. (3), the case temperature can be calculated with Eq. (4).

$$T_c = \begin{pmatrix} T_{c1} \\ T_{c2} \\ \vdots \\ T_{cN} \end{pmatrix} = T_a + \begin{pmatrix} R_{a1} + R_b & r_{12} & \cdots & r_{1N} \\ r_{21} & R_{a2} + R_b & \cdots & r_{2N} \\ \vdots & \vdots & \ddots & \vdots \\ r_{N1} & r_{N2} & \cdots & R_{aN} + R_b \end{pmatrix} \begin{pmatrix} P_{th1} \\ P_{th2} \\ \vdots \\ P_{thN} \end{pmatrix} \tag{4}$$

Optics EXPRESS

The R and r can be derived by FEA stimulation. Taking the Sample LED4 as an example shown in Fig. 5(a), ΔT is temperature difference between the PCB temperature and the ambient, the total P_{th} is the thermal power sum of all LEDs in Sample LED4. R_b is the slope of linear-fitting of (ΔT ~ the total P_{th}). The intercept of linear-fitting of (ΔT ~ the total P_{th}) is assumed as the adjustment factor (T_{ad}) of R_b to maintain the accuracy of PCB temperature. As shown in Fig. 5(b), ΔT_1 is the temperature difference between the case temperature of 1^{st} LED and the temperature of PCB. R_{a1} is the slope of the linear-fitting of (ΔT_1 ~ P_{th} of 1^{st} LED). ΔT_2 is the temperature rise of 2^{nd} LED caused by the energy of 1^{st} LED. r_{12} is the slope of linear-fitting of (ΔT_2 ~ P_{th} of 1^{st} LED).

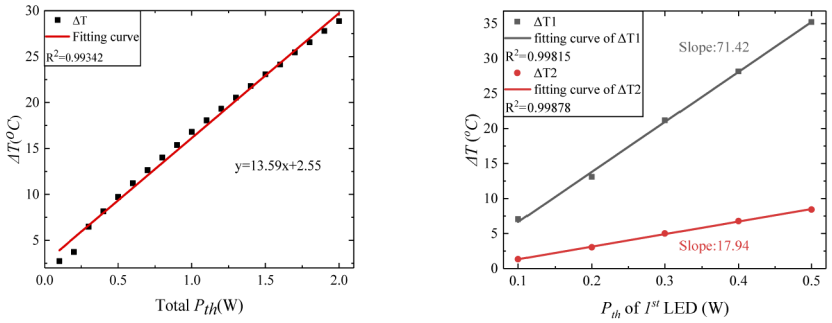

Fig. 5. (a) ΔT v.s. total P_{th} of the Sample LED4 and(b) ΔT_1, ΔT_2 v.s. P_{th} of 1^{st} LED in the Sample LED4

Based on the above analysis, all R, r and T_{ad} can be acquired and the case temperature of the individual LED and LED array can be expressed as Eqs. (5) and Eqs. (6).

$$T_c = T_a + T_{ad} + P_{th}(R_a + R_b) \tag{5}$$

$$T_c = \begin{pmatrix} T_{c1} \\ T_{c2} \\ \vdots \\ T_{cN} \end{pmatrix} = T_a + T_{ad} + \begin{pmatrix} R_{a1} + R_b & r_{12} & \cdots & r_{1N} \\ r_{21} & R_{a2} + R_b & \cdots & r_{2N} \\ \vdots & \vdots & \ddots & \vdots \\ r_{N1} & r_{N2} & \cdots & R_{aN} + R_b \end{pmatrix} \begin{pmatrix} P_{th1} \\ P_{th2} \\ \vdots \\ P_{thN} \end{pmatrix} \tag{6}$$

The case temperatures of Sample LED1, Sample LED4, Sample LED6 and Sample LED9 can be calculated by using the Eqs. (7)–(10) respectively.

$$T_c = 22 + 1.10 + P_{th}(68.69 + 17.57) \tag{7}$$

$$T_c = \begin{pmatrix} T_{c1} \\ T_{c2} \\ T_{c3} \\ T_{c4} \end{pmatrix} = 22 + 2.55 + \begin{pmatrix} 85.01 & 17.94 & 17.67 & 17.78 \\ 17.27 & 84.16 & 17.57 & 16.85 \\ 17.19 & 17.76 & 84.95 & 17.70 \\ 17.19 & 16.94 & 17.59 & 83.97 \end{pmatrix} \begin{pmatrix} P_{th1} \\ P_{th2} \\ P_{th3} \\ P_{th4} \end{pmatrix} \tag{8}$$

Optics EXPRESS

$$T_c = \begin{pmatrix} T_{c1} \\ T_{c2} \\ T_{c3} \\ T_{c4} \\ T_{c5} \\ T_{c6} \end{pmatrix} = 22 + 3.70 + \begin{pmatrix} 83.17 & 15.40 & 13.76 & 13.41 & 14.51 & 15.34 \\ 16.80 & 82.49 & 14.70 & 13.90 & 14.87 & 13.88 \\ 13.60 & 14.80 & 83.14 & 14.91 & 14.01 & 12.95 \\ 13.18 & 14.22 & 13.96 & 70.71 & 15.03 & 13.54 \\ 14.06 & 14.92 & 13.96 & 14.73 & 83.13 & 14.90 \\ 14.96 & 14.12 & 13.08 & 13.39 & 15.11 & 83.07 \end{pmatrix} \begin{pmatrix} P_{th1} \\ P_{th2} \\ P_{th3} \\ P_{th4} \\ P_{th5} \\ P_{th6} \end{pmatrix} \tag{9}$$

$$T_c = \begin{pmatrix} T_{c1} \\ T_{c2} \\ T_{c3} \\ T_{c4} \\ T_{c5} \\ T_{c6} \\ T_{c7} \\ T_{c8} \\ T_{c9} \end{pmatrix} = 22 + 4.53 + \begin{pmatrix} 83.26 & 14.84 & 13.23 & 12.84 & 14.01 & 14.93 & 13.14 & 12.84 & 12.30 \\ 14.76 & 82.65 & 14.73 & 13.85 & 14.80 & 13.97 & 12.79 & 13.06 & 12.79 \\ 13.23 & 14.80 & 82.36 & 14.79 & 14.04 & 12.88 & 12.25 & 12.86 & 13.16 \\ 12.64 & 13.72 & 14.58 & 82.96 & 14.52 & 12.90 & 12.76 & 13.90 & 14.56 \\ 13.96 & 14.81 & 14.00 & 14.64 & 70.18 & 15.50 & 13.60 & 14.73 & 14.36 \\ 14.84 & 13.95 & 12.82 & 13.00 & 14.60 & 83.32 & 14.69 & 13.93 & 12.80 \\ 13.10 & 12.79 & 12.21 & 12.87 & 13.98 & 14.74 & 82.12 & 14.96 & 13.22 \\ 12.17 & 13.04 & 13.40 & 14.81 & 14.72 & 13.93 & 14.90 & 82.38 & 14.63 \\ 12.22 & 12.79 & 13.09 & 14.73 & 13.99 & 12.82 & 13.22 & 14.66 & 83.43 \end{pmatrix} \begin{pmatrix} P_{th1} \\ P_{th2} \\ P_{th3} \\ P_{th4} \\ P_{th5} \\ P_{th6} \\ P_{th7} \\ P_{th8} \\ P_{th9} \end{pmatrix} \tag{10}$$

The temperature distributions of designed test samples were measured by IR camera to verify the prediction accuracy of the proposed TE model. As shown in Fig. 6, the measured maximum case temperatures of Sample LED1 Sample LED4, Sample LED6 and Sample LED9 driven under the current of 125mA are 45.8°C, 62.1°C, 69.7°C, 82.3°C, respectively. Under the same operation condition, when the number of individual LED increases, the case temperature of LED array also increases, which is caused by the thermal coupling effect existing in the LED array. As shown in Fig. 7, the case temperature measurement results under three conditions, with driven currents as 65mA, 125mA and 185mA, were selected to verify the theoretical calculation results with the TE model. For all designed test samples, the theoretically calculated case temperatures are close to the corresponding measured values well under all operation conditions (see Fig. 7), in which the largest mean of prediction error is 2.76% and its variance is 1.58 (see Table 3). This result demonstrates that the proposed TE model with a high prediction accuracy is appropriate to be used in the following TES modeling.

Optics EXPRESS

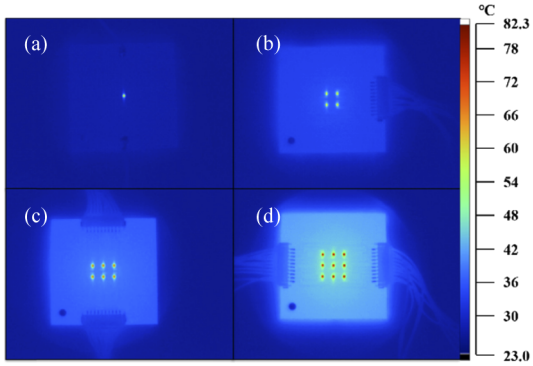

Fig. 6. Infrared measurement results: (a) Sample LED1; (b) Sample LED4; (c) Sample LED6; (d) Sample LED9 driven under the current of 125mA

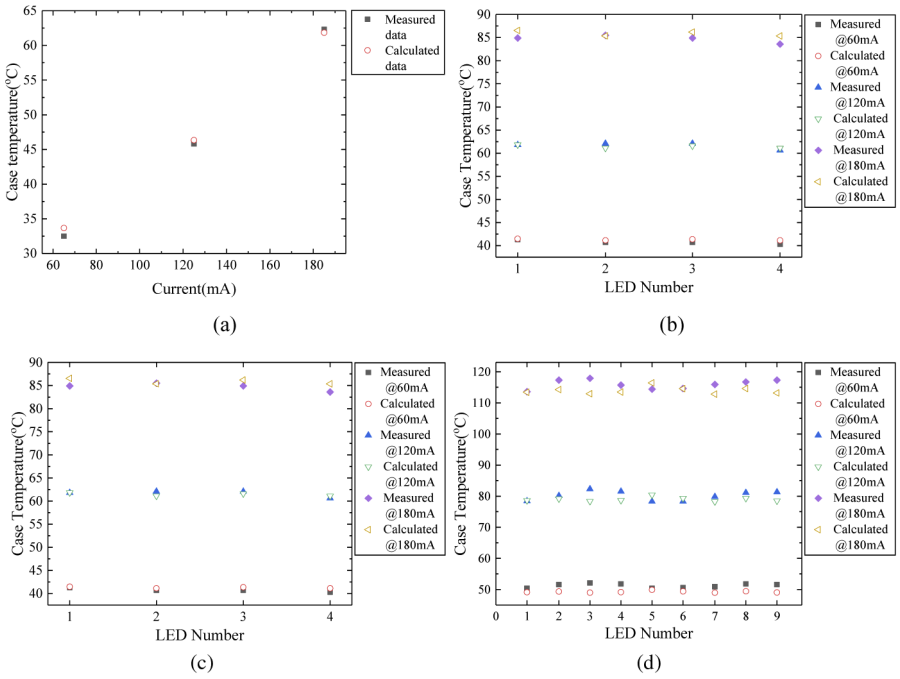

Fig. 7. The case temperature of the samples under different current: (a) Sample LED1; (b) Sample LED4; (c) Sample LED6; (d) Sample LED9.

Table 3. The Means and Variances of Prediction Errors for Different Test Samples

Test samples	Means of prediction errors (%)	Variances of prediction errors
Sample LED1	1.78	1.19
Sample LED4	1.17	0.71
Sample LED6	2.03	0.87
Sample LED9	2.76	1.58

Optics EXPRESS

3.2. Thermal-electrical-spectral modeling

Figure 8 illustrates the flowchart of optical and chromatic performance prediction for LED array. The implement procedure is explained step by step as follows:

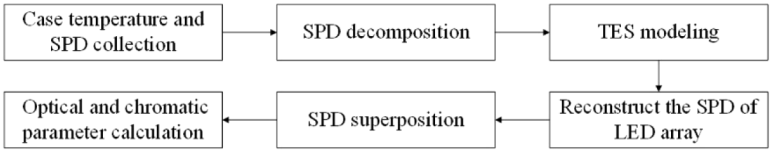

Fig. 8. The flowchart of prediction methodologies

3.2.1. Step 1: Case temperature and SPD collection for the individual LED

Firstly, as shown in Fig. 9(a), the case temperatures of the individual LED (Sample LED1) were measured under different operation conditions by using IR camera. Then, their photoelectricity parameters and and SPDs were measured under same operation condition by using integrating sphere measurement system. Finally, the relationship between the photoelectricity parameters and the current, case temperature were experimentally obtained at this stage. Table 4 lists the experimental schemes for Sample LED1 and the measured case temperatures are showed in Fig. 9(b).

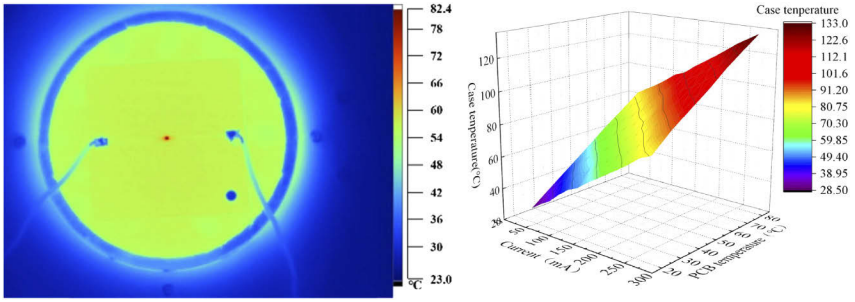

(a) (b)

Fig. 9. (a) The measured temperature distribution of Sample LED1 under the current of 120 mA and the PCB temperature of 60°C and (b) The measured case temperatures of Sample LED1 under different operation conditions

Table 4. Experimental Scheme for Sample LED1

Factors	Schemes
Currents	From 40mA to 280mA with an interval of 20mA
PCB temperatures	From 20°C to 80°C with an interval of 10°C

3.2.2. Step 2: SPD decomposition

The SPD characterizes the relationship between the intensity and the wavelength of an illuminant. Three widespread used statistical functions, such as Gaussian model [40], Asymmetric double sigmoidal (Asym2sig) model [35] and Lorentzian model [34], are proposed to describe the SPD of the LED used in this paper. As for pc-WLED, the SPD always has some bell-shaped peaks that represent the light emitted by the chip and the light converted by mixture of several kinds of

Optics EXPRESS

phosphors. So, the SPD models for a pc-WLED need to be extended as multi-peak functions, as shown from Eq. (11) to Eq. (13):

(1) The extended Gaussian SPD model:

$$SPD_{LED}(\lambda) = a_1 exp\left[-2\left(\frac{\lambda-\lambda_{c1}}{w_1}\right)^2\right] + a_2 exp\left[-2\left(\frac{\lambda-\lambda_{c2}}{w_2}\right)^2\right] \tag{11}$$

(2) The extended Asym2sig SPD model:

$$SPD_{LED}(\lambda) = b_1 \frac{1-\frac{1}{1+exp[-(\lambda-\lambda_{c1})/v_1]}}{1+exp[-(\lambda-\lambda_{c1})/u_1]} + b_2 \frac{1-\frac{1}{1+exp[-(\lambda-\lambda_{c2})/v_2]}}{1+exp[-(\lambda-\lambda_{c2})/u_2]} \tag{12}$$

(3) The extended Lorentzian SPD model:

$$SPD_{LED}(\lambda) = \frac{2a_1}{\pi} \times \frac{w_1}{4(\lambda-\lambda_{c1})+{w_1}^2} + \frac{2a_2}{\pi} \times \frac{w_2}{4(\lambda-\lambda_{c2})+{w_2}^2} \tag{13}$$

where λ is the wavelength; a_1, λ_{c1}, w_1, b_1, u_1 and v_1 are the area, peak wavelength, full width at half maximum (FWHM), the amplitude, variance of the low-energy and variance of the high-energy sides of the blue LED part spectrum, respectively; a_2, λ_{c2}, w_2, b_2, u_2 and v_2 are the area, peak wavelength, full width at half maximum (FWHM), the amplitude, variance of the low-energy and variance of the high-energy sides of the phosphor part spectrum, respectively.

All SPD data of individual LED (Sample LED1) were fitted by the proposed three extended SPD models. As an example, Fig. 10 presents the measured and fitted SPD data of Sample LED1 driven under the current of 120 mA with the case temperature of 64.8°C. The means and variances of R^2 of three extends models, representing the Goodness-of-Fit, are shown in Table 5, which indicates that the extended Asym2sig model with the higher R^2 and the lower variance can be selected in this paper to extract the spectral characteristic parameters for the test samples.

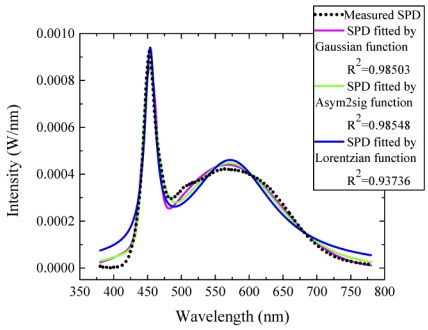

Fig. 10. The measured and fitted SPD data of Sample LED1 driven under the current of 120 mA with the case temperature of 64.8°C

Table 5. The Means and Variances of R^2 of Three Extends Models

SPD models	Means of R^2	Variances of R^2
Extended Gaussian SPD model	0.986061	0.003026
Extended Asym2sig SPD model	0.986359	0.002553
Extended Lorentzian SPD model	0.939333	0.006012

Optics EXPRESS

3.2.3. Step 3: TES modeling

The extracted eight spectral characteristic parameters of the extended Asym2sig model were then modelled as a function of current (I) and case temperature (Tc). According to the Eq. (14), a quadratic polynomial function is proposed as the TES model in this paper to relate the eight spectral characteristic parameters with I and Tc.

Thermal-Electrical-Spectral (TES) model:

$$z(I,T) = p_1 + p_2 I + p_3 T + p_4 I^2 + p_5 IT + p_6 T^2 \tag{14}$$

in which z denotes each spectral characteristic parameter, and p_1 to p_6 are the parameters relevant to the fitted spectral characteristic parameters. The fitted surfaces agree well with the spectral characteristic parameters collected at different conditions and the fitting results of eight spectral characteristic parameters are listed in Table 6. The value (p_1 to p_6) of each spectral characteristic parameter was obtained after fitting. All R^2 values are higher than 0.95, especially for b_1, λ_{c1}, u_1, v_1 and b_2 with R^2 higher than 0.99. This means that the proposed quadratic polynomial based TES model is suitable to dynamically describe the changes of all spectral characteristic parameters for Sample LED1 operated under designed usage conditions.

Table 6. The Fitting Results of Eight Spectral Characteristic Parameters with The Quadratic Polynomial Function

Spectral characteristic parameters	p_1	p_2	p_3	p_4	p_5	p_6	R^2
b_1	-0.00015	2.61e-05	5.92e-06	-9.80e-09	-5.60e-08	-4.43e-08	0.9999
λ_{c1}	446.3	-0.0154	0.0175	2.85e-05	-4.28e-05	0.000210	0.9969
u_1	2.723	0.002938	0.01163	-1.89e-06	-6.74e-06	5.57e-05	0.9993
v_1	9.552	-0.01565	0.03463	2.57e-05	-7.94e-06	4.06e-05	0.9952
b_2	-1.28e-05	1.79e-05	3.04e-06	-1.04e-08	-2.96e-08	-3.02e-08	0.9999
λ_{c2}	565.4	-0.05124	0.08277	0.000154	-0.00051	0.000545	0.9808
u_2	45.9	-0.00757	0.02428	2.47e-05	-9.58e-05	-4.35e-05	0.956
v_2	51.87	0.01075	-0.02877	-4.49e-05	0.000177	-0.00025	0.9696

3.2.4. Step 4: Reconstruction of the SPD of the LED array

The SPD of LED array operated under certain conditions can be reconstructed by using the above proposed TES model. Meanwhile, the TE model is used to estimate the case temperature for each LED individuals in an LED array operated under the certain current and environment temperature. Given the case of powering 1^{st}, 2^{nd}, $3^{rd}$and 4^{th}, 5^{th}, 6^{th} LED in Sample LED6 with the current 180 mA and 60 mA respectively, the calculated case temperature of each LED is 76.88°C, 77.46°C, 77.03°C, 56.79°C, 57. 46°C, 56.78°C in turns. The predicted spectral characteristic parameters of each LED in sample LED6 are listed in Table 7.

Table 7. The Predicted Spectral Characteristic Parameters of Each LED in Sample LED6

LED No.	b_1	λ_{c1}	u_1	v_1	b_2	λ_{c2}	u_2	v_2
1^{st} LED	0.00365	446.45	4.32	10.36	0.00252	563.61	45.62	51.07
2^{nd} LED	0.00364	446.47	4.33	10.39	0.00251	563.65	45.62	51.05
3^{rd} LED	0.00365	446.45	4.32	10.37	0.00252	563.62	45.62	51.06
4^{th} LED	0.00138	447.00	3.71	10.78	0.00100	567.58	46.45	50.49
5^{th} LED	0.00138	447.03	3.72	10.80	0.00100	567.65	46.46	50.46
6^{th} LED	0.00138	447.00	3.71	10.78	0.00100	567.58	46.45	50.49

Optics EXPRESS

3.2.5. Step 5: SPD superposition

For an LED array, its SPD can be composed of the SPDs of all LED individuals, as shown in Eq. (15).

$$SPD_{ARR}(\lambda) = \sum_{i=1}^{n} SPD_{LED\,i}(\lambda) \tag{15}$$

where $SPD_{ARR}(\lambda)$ is the SPD of an LED array, $SPD_{LED\,i}(\lambda)$ is the SPD of i^{th} LED in this LED array. As shown in Fig. 11(a), the predicted SPD of Sample LED6 by summing of the SPD of each LED is basically consistent with the measured one.

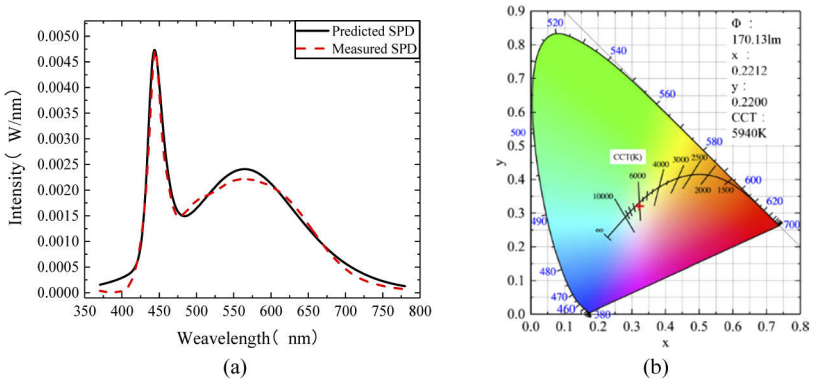

Fig. 11. (a) Superposition SPD of sample LED6 and verified by the measured SPDand (b) The predicted optical and chromatic parameters of Sample LED6

3.2.6. Step 6: Optical and chromatic parameter calculation

Normally, the SPD is an intermediate to calculate the optical and chromatic characteristics according to the Commission Internationale de L'Eclairage (CIE) definitions, such as luminous flux, CCT, chromaticity coordinate. The optical and chromatic parameters of Sample LED6 operated under the condition mentioned in step 4 are predicted and shown in Fig. 11(b).

4. Model validation with case study

To verify the proposed TES model, four test samples designed in Fig. 1(b) operated under three different conditions, including all LEDs powered-on with same current, parts of LEDs powered-on with same current and LEDs powered-on with different currents, were considered in this part. Those power supply modes are popular in the actual operations of LED array.

4.1. Case 1: all LEDs powered-on with same current

Three currents, i.e. 65 mA, 125 mA and 185 mA, are selected to power-on all LEDs in four test samples, thus, there are totally 12 operation conditions in this case as list in Table 8. The prediction results of optical and chromatic parameters are shown in Fig. 12. There is no obvious tendency for luminous flux and CCT, however, the predicted chromaticity coordinate x and y are lower than those measured values. Overall the absolute prediction errors of luminous flux, CCT, chromaticity coordinate x and y are lower than 5%.

4.2. Case 2: parts of LEDs powered-on with same current

At some time, only parts of LEDs in an array are powered-on, such as transferring the high beam to low beam for an automotive headlamp. This case is also considered and verified in this study

Optics EXPRESS

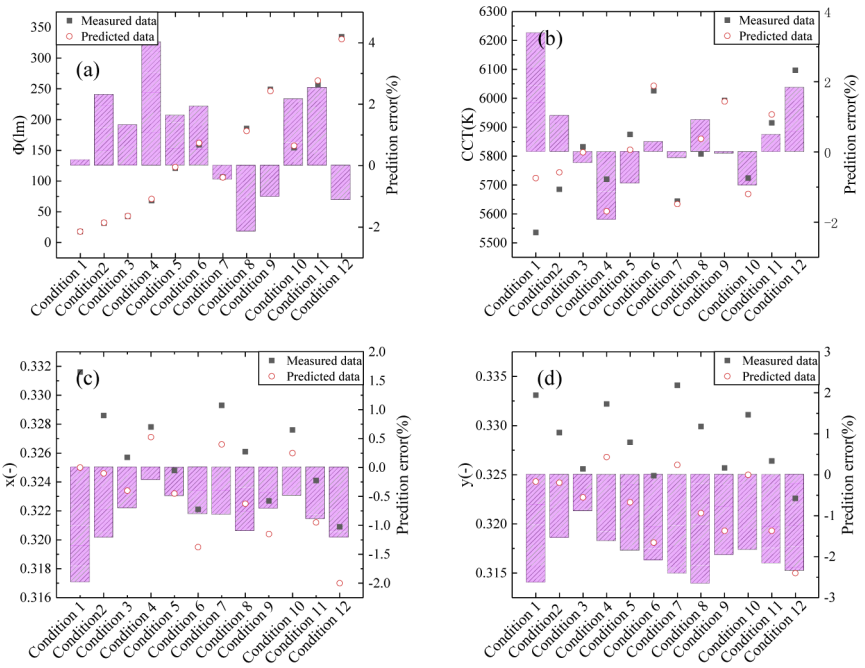

Fig. 12. The prediction results of optical and chromatic parameters when all LEDs powered-on with same current: (a)luminous flux; (b)CCT; (c) chromaticity coordinate *x*; (d) chromaticity coordinate *y*

Table 8. The Operation Conditions for All Test Samples When All LEDs Powered-on with Same Current

Condition No.	Brief describes
Condition 1	Sample LED1: power-on with 65mA
Condition 2	Sample LED1: power-on with 125mA
Condition 3	Sample LED1: power-on with 185mA
Condition 4	Sample LED4: power-on with 65mA
Condition 5	Sample LED4: power-on with 125mA
Condition 6	Sample LED4: power-on with 185mA
Condition 7	Sample LED6: power-on with 65mA
Condition 8	Sample LED6: power-on with 125mA
Condition 9	Sample LED6: power-on with 185mA
Condition 10	Sample LED9: power-on with 65mA
Condition 11	Sample LED9: power-on with 125mA
Condition 12	Sample LED9: power-on with 185mA

and different operation conditions are shown in Table 9. As shown in Fig. 13, There is also no obvious tendency for luminous flux and CCT, however, the predicted chromaticity coordinate *x* and *y* are lower than those measured values. The prediction results show good agreement with the actual measurements, and the prediction error can be controlled under 4%.

Optics EXPRESS

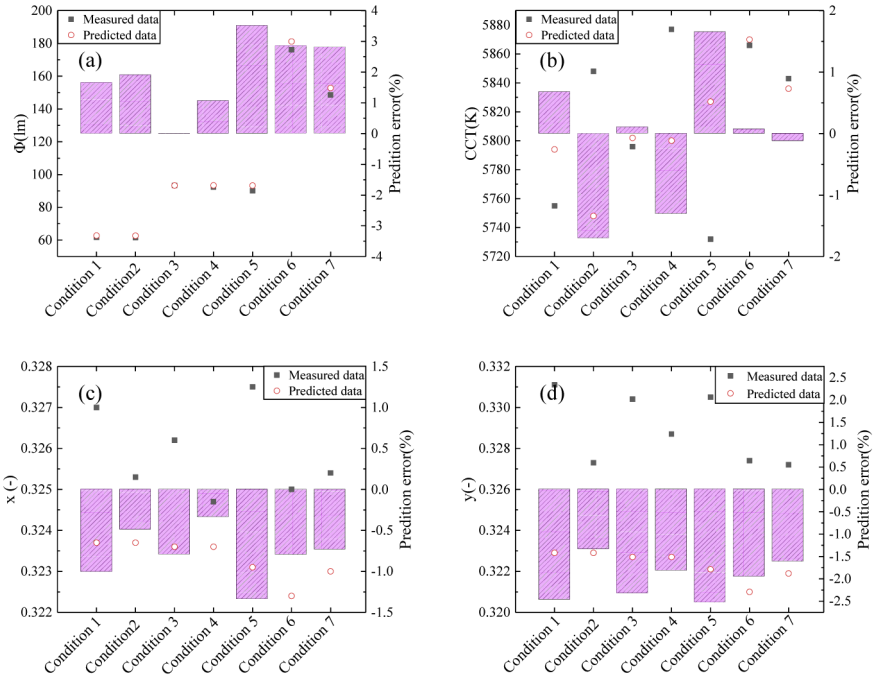

Fig. 13. The prediction results of optical and chromatic parameters when parts of LEDs powered-on with same current: (a)luminous flux; (b)CCT; (c) chromaticity coordinate *x*; (d) chromaticity coordinate *y*

Table 9. The Operation Conditions for All Test Samples When Parts of LEDs Powered-on with Same Current

Condition No.	Brief describes
Condition 1	Sample LED4: powering 1^{st}, 2^{nd} LED
Condition 2	Sample LED4: powering 1^{st}, 3^{rd} LED
Condition 3	Sample LED6: powering 1^{st}, 2^{nd}, 3^{th} LED
Condition 4	Sample LED6: powering 1^{st}, 3^{rd}, 5^{th} LED
Condition 5	Sample LED9: powering 1^{st}, 2^{nd}, 3^{rd} LED
Condition 6	Sample LED9: powering 1^{st}, 3^{rd}, 5^{th}, 7^{th}, 9^{th} LED
Condition 7	Sample LED9: powering 1^{st}, 2^{nd}, 3^{rd}, 4^{th}, 5^{th}, 6^{th} LED

Optics EXPRESS

4.3. Case 3: LEDs powered-on with different currents

To get different lighting effects, it is necessary to individually control the luminous intensities of different LEDs in an LED array, therefore it is valuable to discuss the case of powering LEDs with different currents. The selected operation conditions are listed in Table 10. The corresponding results shown in Fig. 14 also present the high prediction accuracies of four optical and chromatic parameters with the absolute prediction error under 4%.

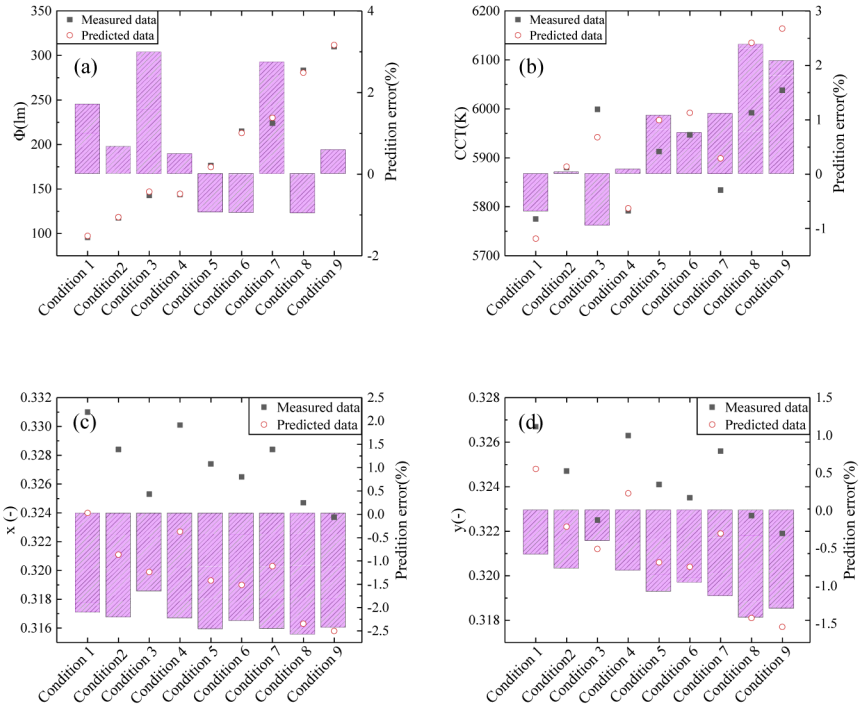

Fig. 14. The prediction results of optical and chromatic parameters when LEDs powered-on with different currents: (a)luminous flux; (b)CCT; (c) chromaticity coordinate x; (d) chromaticity coordinate y

Table 10. The Operation Conditions for All Test Samples When LEDs Powered-on With Different Currents

Condition No.	Brief describes
Condition 1	Sample LED4: 1^{st}, 2^{nd} with 125mA; 3^{rd}, 4^{th} with 65mA
Condition 2	Sample LED4: 1^{st}, 2^{nd} with 185mA; 3^{rd}, 4^{th} with 65mA
Condition 3	Sample LED4: 1^{st}, 2^{nd} with 185mA; 3^{rd}, 4^{th} with 125mA
Condition 4	Sample LED6: 1^{st}, 2^{nd}, 3^{rd} with 125mA; 4^{th}, 5^{th}, 6^{th} with 65mA
Condition 5	Sample LED6: 1^{st}, 2^{nd}, 3^{rd} with 185mA; 4^{th}, 5^{th}, 6^{th} with 65mA
Condition 6	Sample LED6: 1^{st}, 2^{nd}, 3^{rd} with 185mA; 4^{th}, 5^{th}, 6^{th} with 125mA
Condition 7	Sample LED9: 1^{st}, 2^{nd}, 3^{rd}, 7^{th}, 8^{th}, 9^{th} with 125mA; 4^{th}, 5^{th}, 6^{th} with 65mA
Condition 8	Sample LED9: 1^{st}, 2^{nd}, 3^{rd}, 7^{th}, 8^{th}, 9^{th} with 185mA; 4^{th}, 5^{th}, 6^{th} with 65mA
Condition 9	Sample LED9: 1^{st}, 2^{nd}, 3^{rd}, 7^{th}, 8^{th}, 9^{th} with 185mA; 4^{th}, 5^{th}, 6^{th} with 125mA

Optics EXPRESS

5. Conclusion

In this paper, a TES model integrating the TE model considering the thermal coupling effect with the SPD decomposition model is proposed to achieve the dynamic prediction of optical and chromatic performances for LED array. Meanwhile, a series of case temperature and SPD measurement experiments are conducted to build and verify the proposed TES model. The results indicate that: (1) the proposed TE model is feasible to describe the thermal coupling effect in an LED array, and this model has a high case temperature prediction accuracy for the LED array; (2) the quadratic polynomial based TES model is suitable to dynamically describe the changes of all spectral characteristic parameters of an individual LED operated under usage conditions; (3) the TES model can be used to predict the optical and chromatic parameters for LED arrays, and three case studies considering the actual usages in automotive headlamp LED arrays validate the proposed TES model with the prediction accuracy higher than 95%. Therefore, it is useful in developing new intelligent automotive headlamps by taking the electrical-thermal-optical balance and optimization into consideration.

Funding

National Natural Science Foundation of China (51805147, 61673037); Six Talent Peaks Project in Jiangsu Province (GDZB-017); the Key R&D Plan of Jiangsu Province (BE2019041).

Disclosures

The authors declare no conflicts of interest.

References

1. M. Hamidnia, Y. Luo, and X. D. Wang, "Application of micro/nano technology for thermal management of high power LED packaging – A review," Appl. Therm. Eng. **145**, 637–651 (2018).
2. Q. Wang, H. Xu, F. Zhang, and Z. Wang, "Influence of color temperature on comfort and preference for LED indoor lighting," Optik **129**, 21–29 (2017).
3. T. Ouzounis, E. Heuvelink, Y. Ji, H. J. Schouten, R. G. F. Visser, and L. F. M. Marcelis, "Blue and red LED lighting effects on plant biomass, stomatal conductance, and metabolite content in nine tomato genotypes," Acta Hortic. **1134**(1134), 251–258 (2016).
4. Z. Lu, P. Bai, B. Huang, A. Henzen, R. Coehoorn, H. Liao, and G. Zhou, "Experimental investigation on the thermal performance of three-dimensional vapor chamber for LED automotive headlamps," Appl. Therm. Eng. **157**, 113478 (2019).
5. M. Roncati, D. Lauritano, F. Cura, and F. Carinci, "Evaluation of light-emitting diode (LED-835 NM) application over human gingival fibroblast: an in vitro study," Journal of Biological Regulators & Homeostatic Agents **30**, 161 (2016).
6. Y. Chien-Hung, L. Yen-Liang, and C. Chi-Wai, "Real-time white-light phosphor-LED visible light communication (VLC) with compact size," Opt. Express **21**(22), 26192–26197 (2013).
7. I. E. Fragkos, V. Dierolf, Y. Fujiwara, and N. Tansu, "Physics of Efficiency Droop in GaN:Eu Light-Emitting Diodes," Sci. Rep. **7**(1), 16773 (2017).
8. Y. Lee, C. Chen, and C. Lee, "Reduction in the Efficiency-Droop Effect of InGaN Green Light-Emitting Diodes Using Gradual Quantum Wells," IEEE Photonics Technol. Lett. **22**(20), 1506–1508 (2010).
9. H. Y. Ryu, K. S. Jeon, M. G. Kang, H. K. Yuh, Y. H. Choi, and J. S. Lee, "A comparative study of efficiency droop and internal electric field for InGaN blue lighting-emitting diodes on silicon and sapphire substrates," Sci. Rep. **7**(1), 44814 (2017).
10. K. Ben Abdelmlek, Z. Araoud, K. Charrada, and G. Zissis, "Optimization of the thermal distribution of multi-chip LED package," Appl. Therm. Eng. **126**, 653–660 (2017).
11. H. Tang, H. Ye, X. Chen, C. Qian, X. Fan, and G. Zhang, "Numerical Thermal Analysis and Optimization of Multi-Chip LED Module Using Response Surface Methodology and Genetic Algorithm," IEEE Access **5**, 16459–16468 (2017).
12. J. Zhou, J. Huang, Y. Wang, and Z. Zhou, "Thermal distribution of multiple LED module," Appl. Therm. Eng. **93**, 122–130 (2016).
13. G. Elger, B. Spinger, N. Bienen, and N. Benter, "LED Matrix light source for adaptive driving beam applications," in *IEEE Electronic Components & Technology Conference* (2013).

Optics EXPRESS

14. W. Chen, J. Fan, C. Qian, B. Pu, X. Fan, and G. Zhang, "Reliability Assessment of Light-Emitting Diode Packages With Both Luminous Flux Response Surface Model and Spectral Power Distribution Method," IEEE Access **7**, 68495–68502 (2019).
15. C. Xiao, H. Liao, Y. Wang, J. Li, and W. Zhu, "A novel automated heat-pipe cooling device for high-power LEDs," Appl. Therm. Eng. **111**, 1320–1329 (2017).
16. J. Wang, Y.-x. Cai, W.-w. Bao, H.-x. Li, and Q. Liu, "Experimental study of high power LEDs heat dissipation based on corona discharge," Appl. Therm. Eng. **98**, 420–429 (2016).
17. M. W. Jeong, S. W. Jeon, and Y. Kim, "Optimal thermal design of a horizontal fin heat sink with a modified-opening model mounted on an LED module," Appl. Therm. Eng. **91**, 105–115 (2015).
18. K. C. Yung, H. Liem, H. S. Choy, and Z. X. Cai, "Thermal investigation of a high brightness LED array package assembly for various placement algorithms," Appl. Therm. Eng. **63**(1), 105–118 (2014).
19. H. Lu, Y. Lu, L. Zhu, Y. Lin, Z. Guo, T. Liu, Y. Gao, G. Chen, and Z. Chen, "Efficient Measurement of Thermal Coupling Effects on Multichip Light-Emitting Diodes," IEEE Trans. Power Electron. **32**(12), 9280–9292 (2017).
20. J. Kang, J. Choi, D. Kim, J. Kim, Y. Song, G. Kim, and S. Han, "Fabrication and Thermal Analysis of Wafer-Level Light-Emitting Diode Packages," IEEE Electron Device Lett. **29**(10), 1118–1120 (2008).
21. T. Treurniet and V. Lammens, "Thermal management in color variable multi-chip led modules," in *Twenty-Second Annual IEEE Semiconductor Thermal Measurement And Management Symposium* (2006), pp. 173–177.
22. H. Zou, L. Lu, J. Wang, B. Shieh, and S. W. R. Lee, "Thermal characterization of multi-chip light emitting diodes with thermal resistance matrix," in *2017 14th China International Forum on Solid State Lighting: International Forum on Wide Bandgap Semiconductors China (SSLChina: IFWS)* (2017), pp. 32–37.
23. S. Y. Hui and Y. X. Qin, "A General Photo-Electro-Thermal Theory for Light Emitting Diode (LED) Systems," IEEE Trans. Power Electron. **24**(8), 1967–1976 (2009).
24. S. Y. R. Hui, H. Chen, and X. Tao, "An Extended Photoelectrothermal Theory for LED Systems: A Tutorial From Device Characteristic to System Design for General Lighting," IEEE Trans. Power Electron. **27**(11), 4571–4583 (2012).
25. H. T. Chen, X. H. Tao, and S. Y. R. Hui, "Estimation of Optical Power and Heat-Dissipation Coefficient for the Photo-Electro-Thermal Theory for LED Systems," IEEE Trans. Power Electron. **27**(4), 2176–2183 (2012).
26. H. Chen, A. T. L. Lee, S. Tan, and S. Y. Hui, "Dynamic Optical Power Measurements and Modeling of Light-Emitting Diodes Based on a Photodetector System and Photo-Electro-Thermal Theory," IEEE Trans. Power Electron. **34**(10), 10058–10068 (2019).
27. A. Lee, H. Chen, S. C. Tan, and S. Y. R. Hui, "Dynamic Photo-Electro-Thermal Modeling of Light-Emitting Diodes with Phosphor Coating as Light Converter," IEEE Journal of Emerging and Selected Topics in Power Electronics, 1 (2018).
28. B.-J. Huang and C.-W. Tang, "Thermal–electrical–luminous model of multi-chip polychromatic LED luminaire," Appl. Therm. Eng. **29**(16), 3366–3373 (2009).
29. C.-H. Lin, C.-H. Huang, Y.-M. Pai, C.-F. Lee, C.-C. Lin, C.-W. Sun, C.-H. Chen, C.-W. Sher, and H.-C. Kuo, "Novel Method for Estimating Phosphor Conversion Efficiency of Light-Emitting Diodes," Crystals 8 (2018).
30. B. Sun, J. Fan, X. Fan, and G. Zhang, "A SPICE-based Transient Thermal-Electronic Model for LEDs," in *2019 20th International Conference on Thermal, Mechanical and Multi-Physics Simulation and Experiments in Microelectronics and Microsystems (EuroSimE)* (2019), pp. 1–5.
31. C. Negrea, P. Svasta, and M. Rangu, "Electro-thermal modeling of power LED using SPICE circuit solver," in *2012 35th International Spring Seminar on Electronics Technology* (2012), pp. 329–334.
32. K. Górecki and P. Ptak, "Modelling LED lamps in SPICE with thermal phenomena taken into account," Microelectron. Reliab. **79**, 440–447 (2017).
33. P. Baureis, "Compact modeling of electrical, thermal and optical LED behavior," in *Proceedings of 35th European Solid-State Device Research Conference*, *2005. ESSDERC 2005* (2005), pp. 145–148.
34. J. Fan, M. G. Mohamed, C. Qian, X. Fan, G. Zhang, and M. Pecht, "Color Shift Failure Prediction for Phosphor-Converted White LEDs by Modeling Features of Spectral Power Distribution with a Nonlinear Filter Approach," Materials **10**(7), 819 (2017).
35. C. Qian, J. Fan, X. Fan, and G. Zhang, "Prediction of Lumen Depreciation and Color Shift for Phosphor-Converted White Light-Emitting Diodes Based on A Spectral Power Distribution Analysis Method," IEEE Access **5**, 24054–24061 (2017).
36. H. T. Chen, D. Y. Lin, S. C. Tan, and S. Y. R. Hui, "Chromatic, Photometric and Thermal Modeling of LED Systems with Non-Identical LED Devices," in *IEEE Trans. Power Electron.* (2014), pp. 6636–6647.
37. H. Chen and S. Y. Hui, "Dynamic Prediction of Correlated Color Temperature and Color Rendering Index of Phosphor-Coated White Light-Emitting Diodes," IEEE Transactions on Industrial Electronics **61**(2), 784–797 (2014).
38. Y. E. Huaiyu, S. W. Koh, C. Yuan, H. van Zeijl, A. W. J. Gielen, S. W. R. Lee, and G. Zhang, "Electrical—thermal—luminous—chromatic model of phosphor-converted white light-emitting diodes," Appl. Therm. Eng. **63**(2), 588–597 (2014).
39. K. F. Han, P. P. Yi, P. Y. Shang, T. T. Chen, C. P. Wang, C. L. Chen, and T. C. Pei, "The evaluation for the chromatic characteristics of LED module under electrical and thermal coupling analysis," Microelectron. Reliab. **53**(12), 1916–1921 (2013).
40. H. Guoxing and Y. Huafeng, "Optimal spectra of the phosphor-coated white LEDs with excellent color rendering property and high luminous efficacy of radiation," Opt. Express **19**(3), 2519–2529 (2011).